SYMPLECTIC MAPPINGS

JOHN D. HADJIDEMETRIOU
University of Thessaloniki, Department of Physics
GR-540 06 Thessaloniki, Greece
e-mail: hadjidem@olymp.ccf.auth.gr

Abstract. This paper reviews the main methods for constructing mapping models for Hamiltonian systems, for the study of motion in the Solar System. The emphasis is given to the relation between the various mapping techniques, the methods to check how close is a mapping model to the original system and the effects of an incomplete model on the evolution of the system.

1. Introduction

The evolution of a subsystem in the Solar System, as for example the motion of an asteroid under the gravitational attraction of the Sun and Jupiter, can be described by a Hamiltonian system. It is known that the flow in the $2n$-dimensional phase space, from an initial position (q_0, p_0) at time $t = t_0$ to the position (q_1, p_1) at the time $t = t_1$ is a canonical transformation, where n is the number of degrees of freedom and q, p are n-vectors. This means that the mapping in phase space from the time t_0 to the time t_1 is a symplectic mapping. [1] An important property of a symplectic map is that it conserves the volume in phase space.

A very useful tool in the study of a Hamiltonian system is the method of Poincaré map on a surface of section. The continuous flow in the $2n$-dimensional phase space is reduced to a map in a $(2n-2)$-dimensional phase space. The Poincaré map is also symplectic. This method is especially useful in systems with two degrees of freedom, where instead of studying the flow

[1] A map $T : M \to M$ is symplectic if its Jacobian matrix $L = DT$ satisfies the symplectic property $L^T J L = J$, where J is the symplectic matrix with rows (in block form) $(0, I)$ and $(-I, 0)$, (I and 0 are the $n \times n$ unit and zero matrices, respectively) and L^T is the transpose of L.

S. Ferraz-Mello et al. (eds.), Dynamics, Ephemerides and Astrometry of the Solar System, 255–266.

in a 4-dimensional phase space we study the map in a 2-dimensional space. The fixed points of the Poincaré map coincide with the periodic orbits of the system and it is clear that their position and stability character determine the topology of the reduced phase space.

By making use of the Poincaré surface of section we do not lose any information: the map describes completely the system. However, in order to find the Poincaré map we must solve the system of differential equations which, in general, cannot be solved in a closed form, because the system is nonintegrable. Thus the only way to obtain the Poincaré map is to use numerical integrations.

2. Construction of mapping models

As mentioned above, the Poincaré map involves the solution of a nonintegrable dynamical system. In order to overcome this difficulty, we can construct mapping models to study the evolution of the Hamiltonian system. There are several methods to do this, that will be explained in the following. All of them are based on a perturbation method and consequently the series may not converge beyond a certain value of a small parameter.

In order for a mapping model to be realistic, its phase space must have the same topology as that of the Poincaré map of the original Hamiltonian system. The *necessary conditions* for a realistic mapping model are:

1. The mapping must be symplectic.
2. The mapping model must have the same fixed points as the Poincaré map.
3. The fixed points must have the correct stability character.

Note that it is not difficult to check the correct position and stability of the fixed points of the mapping model, because they must coincide with the periodic orbits of the original Hamiltonian system and it is relatively easy to compute the main families of periodic orbits of a Hamiltonian system. This provides us with an efficient check of the validity of the mapping model and also of the convergence of the perturbation series involved in the construction of the mapping model.

3. The averaging method

Some important methods for the construction of a mapping model for a nearly integrable dynamical system are based on the method of averaging. For this reason we shall comment on this method and we shall discuss its relation to the original system on one hand and to the corresponding mapping model on the other.

We consider a Hamiltonian system with n degrees of freedom,

$$H = H_0 + \epsilon H_1 \tag{1}$$

where H_0 is the integrable part and ϵ a small parameter. We transform first to action-angle variables, θ, I, of the integrable part and H_0 becomes a function of the actions only, $H_0(I)$. We assume that we are close to a resonance (of H_0) and transform further to new canonical resonant action-angle variables. In this way we have *fast* and *slow* angles. Next, by a new canonical transformation through a suitable generating function, we eliminate the fast angles and we are left with a new, *averaged* Hamiltonian $\bar{H}$ with $(n-1)$ degrees of freedom. It is in this last step that the perturbation method enters and several things could go wrong, because the perturbation series may not converge beyond a certain value of the small parameter (in fact this is always the case).

From the theory of averaging it is known that the fixed points of the averaged Hamiltonian $\bar{H}$ coincide with the periodic orbits of H (or the fixed points of the Poincaré map of H). If H were integrable, the perturbation method would converge and the fixed points of $\bar{H}$ would be identical with the fixed points of the original system (Poincaré map). In a nonintegrable Hamiltonian however the fixed points of $\bar{H}$ may be in the wrong position, or may have the wrong stability, or more fixed points may appear, or some fixed points may be missing. In all these cases the topology of the mapping model is different from that of the real system and consequently the model is not realistic. We shall discuss all these problems in the study of actual dynamical systems in the Solar System that follows.

4. Methods to construct mapping models

We can separate the methods to obtain a mapping model for a Hamiltonian system of the form (1) into two main categories:

A- Solve *approximately* the differential equations of motion and then use the approximate solution to obtain a mapping model.

B- Construct *analytically* the Poincaré map of the integrable part H_0 and express it by a generating function. Then perturb the generating function to obtain the mapping model.

Before we present applications of these methods to the study of actual systems in the solar system, we shall describe the method A, as applied by Wisdom and the method B, as applied by Hadjidemetriou by a simple example, and we shall discuss their similarities and also their relation to the actual system they are designed to represent. Both methods are based on an averaged Hamiltonian $\bar{H}$ of the original Hamiltonian H of the form (1). Other mapping techniques will be also presented. A review on mapping techniques has been presented by Froeschlé (1991).

5. A comparison of the methods A and B by a simple example

5.1. METHOD A

We consider the time dependent Hamiltonian system

$$H = H_0(I) + (K_0/2\pi)\cos(\theta) + H_{hf}(\theta, I, t), \tag{2}$$

where K_0 is a constant, I is the action, θ the angle and

$$H_{hf} = \sum_{n\neq 0} K_n(I)\cos(\theta - nt) \tag{3}$$

is a 2π-periodic function of the time that represents the high frequency terms. By making use of the averaging method (see for example Hadjidemetriou 1991), we obtain the averaged Hamiltonian

$$\bar{H} = H_0(\bar{I}) + (K_0/2\pi)\cos(\bar{\theta}), \tag{4}$$

where $\bar{I}$, $\bar{\theta}$ are the averaged variables. On going from H to $\bar{H}$ we lose information (the time dependence is eliminated with the high frequency terms, which means that in fact we lose one degree of freedom).

We *reintroduce* now the high frequency terms that were eliminated in the averaging process (but not the same terms!). Instead of H_{hf} we add to $\bar{H}$ the high frequency terms (also with period 2π)

$$H^*_{hf} = \sum_{n\neq 0} (K_0/2\pi)\cos(\bar{\theta} - nt) \tag{5}$$

and we have now the Hamiltonian (dropping overbars)

$$H = H_0(I) + K_0\cos(\theta)\,\delta_{2\pi}(t), \tag{6}$$

that will be used in place of the original Hamiltonian (2), where

$$\delta_{2\pi}(t) = \frac{1}{2\pi}\left(1 + 2\sum_{n=1}^{\infty}\cos(nt)\right)$$

is the 2π-periodic delta function.

Note that this is equivalent to substituting $\cos(\bar{\theta})$ in (4) by the sum

$$\sum_{n=-\infty}^{\infty}\cos(\bar{\theta} - nt) = \cos(\bar{\theta})\left(1 + 2\sum_{n=1}^{\infty}\cos(nt)\right) = 2\pi\cos(\bar{\theta})\delta_{2\pi}(t), \tag{7}$$

i.e. we replace $\cos(\theta)$ by 2π-periodic impulses, multiplied by 2π.

https://doi.org/10.1017/S0074180900127500 Published online by Cambridge University Press

The Hamiltonian (6) can be easily solved because it is equal to $H_0(I)$ in all open intervals $(0, 2\pi), (2\pi, 4\pi), \ldots$ The solution from 0^- to $2\pi^-$ gives the mapping for one period 2π of the forcing high frequency term (3). This mapping is:

$$I_1 = I_0 + K_0 \sin(\theta_0), \quad \theta_1 = \theta_0 + 2\pi\, \omega_0(I_1), \tag{8}$$

where $\omega_0(I) \equiv \partial H_0/\partial I$. It can be readily verified that this mapping is symplectic and can be obtained by the generating function

$$F(\theta_0, I_1) = I_1\theta_0 + 2\pi\,[H_0(I_1) + (K_0/2\pi)\cos(\theta_0)]\,. \tag{9}$$

We ask now the question what is the relation between the map (8) and the original system (2). In order for the map (8) to be a realistic model, it must coincide with the Poincaré map of H, i.e. its fixed points should coincide with the fixed points of the Poincaré map, both in position and in stability properties. We remind now that the fixed points of the Poincaré map coincide with the fixed points of the averaged Hamiltonian $\bar{H}$ (provided that $\bar{H}$ is a good model!). So, finally, the comparison between the fixed points of the map (8) and of $\bar{H}$ will provide us the test whether (8) is a realistic model for the original Hamiltonian H.

The fixed points $(\theta_0, I_0$ of the averaged Hamiltonian $\bar{H}$, given by (4), are obtained from the equations

$$\sin(\theta_0) = 0, \quad \omega_0(I_0) = 0. \tag{10}$$

The stability index of the corresponding periodic orbit of the original Hamiltonian (2), which has the period 2π of the forcing term H_{hf}, defined as the sum of the eigenvalues of the monodromy matrix, is

$$k = \exp 2\pi\sqrt{\beta} + \exp -2\pi\sqrt{\beta}, \tag{11}$$

where

$$\beta = (K_0/2\pi)\omega_{0I}(I_0)\cos(\theta_0), \tag{12}$$

and $\omega_{0I} \equiv \partial\omega_0/\partial I$, (Hadjidemetriou, 1991).

The fixed points of the mapping (8) are also given by the equations (10), but the stability index (defined as the sum of the eigenvalues of the linearized mapping at the fixed point) is different and is given by

$$k = 2 + 2\pi K_0\omega_{0I}(I_0)\cos(\theta_0). \tag{13}$$

From the above analysis it is clear that the position of the fixed points is the same in both the averaged Hamiltonian and the corresponding mapping, but the stability index is different, in general. However, the two stability

indices are close if $K_0 << 1$, as can be seen by expanding the exponentials in (11) in powers of $\sqrt{\beta}$:

$$k = 2 + 2\pi K_0 \omega_{0I}(I_0)\cos(\theta_0) + O(K_0^2). \tag{14}$$

Thus, for small K_0 the mapping model is a realistic model for the original system (2).

5.2. THE METHOD B

In this method we solve first the integrable part of $H_0(I)$ of H assuming that K_0 is small, so that the second term in the right hand side of (4) to be considered as a perturbation. The solution is $I = I_0$, $\theta = \omega_0(I_0)t$ and this gives the Poincaré map, at integral multiples of the period 2π:

$$I_1 = I_0, \quad \theta_1 = \theta_0 + 2\pi\omega_0(I_0). \tag{15}$$

This is obtained from the generating function

$$F_0(I_1, \theta_0) = I_1\theta_0 + 2\pi H_0(I_1) \tag{16}$$

through the equations $I_0 = \partial F_0/\partial\theta_0$, $\theta_1 = \partial F_0/\partial I_1$. We perturb now the generating function (16) in such a way that the new map has the same topology as the Poincaré map of the original system. Note that this map is *always* symplectic by its construction. It can be proved (Hadjidemetriou, 1991,1993) that this can be achieved by adding a perturbation term F_1 to F_0, which is the perturbation term of $\bar{H}$, given by (4), multiplied by the period 2π,

$$F_1 = K_0\cos(\theta). \tag{17}$$

Thus, the generating function is $F = F_0 + F_1$ and we can verify that it coincides with the generating function (9) of the mapping (8).

5.3. COMPARISON OF METHODS A AND B

From the previous two sections we come to the conclusion that both methods A and B are equivalent, for the simple example we used to demonstrate these methods, provided $K_0 << 1$. This may not be always the case. Method B gives always a symplectic map, and it can be proved that it gives mapping models that are realistic (i.e they satisfy the necessary conditions of section 2), provided of course that the averaged Hamiltonian on which they are based are realistic. The map however that is obtained with method A may not be symplectic (Henrard, 1995), as can be seen by considering K_0 in (2) as a function of I, $K_0 = K_0(I)$. The mapping obtained by the method A is

$$I_1 = I_0 + K_0(I_0)\sin(\theta_0), \quad \theta_1 = \theta_0 + 2\pi\omega_0(I_1) + K'(I_0)\cos(\theta_0),$$

which is not symplectic, while the mapping obtained by method B is

$$I_1 = I_0 + K_0(I_1)\sin(\theta_0), \quad \theta_1 = \theta_0 + 2\pi\omega_0(I_1) + K'(I_1)\cos(\theta_0),$$

which is symplectic.

Finally, we remark that the above two methods that were demonstrated by a simple example, can be extended to systems with more degrees of freedom, as we shall see in the applications that follow.

6. Application of mapping methods in the Solar System

6.1. RESONANT ASTEROID MOTION: THE WISDOM MAPPING

The method described in section 5.1 to obtain a mapping model for a Hamiltonian system has been applied by Wisdom (1982,1983,1985) for the study of an asteroid at the 3:1 resonance with Jupiter. The underlying dynamical system is the planar elliptic restricted three body problem, with the Sun and Jupiter as primaries. The averaged Hamiltonian used to obtain the mapping model is

$$\begin{aligned} H &= -\frac{\mu_1^2}{2\Phi^2} - 3\Phi + \mu F(x^2+y^2) \\ &\quad + e_j\mu G x - \mu\left[C(x_2 - y_2) + e_j D + e_j^2 E\right]\cos\phi \\ &\quad - \mu\left[2Cxy + e_j D y\right]\sin\phi, \end{aligned} \tag{18}$$

where $\mu_1 = 1-\mu$, $\Phi = \sqrt{\mu_1 a}$, $\phi = l - 3l_j$ and

$$x = \sqrt{2\rho}\cos\omega, \quad y = \sqrt{2\rho}\sin\omega, \tag{19}$$

with $\rho = \sqrt{\mu_1 a}\left(1 - \sqrt{1-e^2}\right)$. The semimajor axis of the asteroid is a, its eccentricity is e, its mean longitude is l, the argument of perihelion is ω, the subscript j refers to Jupiter and μ is the mass of Jupiter. The angle ϕ is the resonant angle (*slow* angle). The averaged Hamiltonian (18) is obtained from the Hamiltonian of the elliptic restricted three body problem by eliminating the high frequency terms, which in this case is the orbital motion of Jupiter in its orbit around the Sun, with period 2π. The high frequency terms are reintroduced by 2π-periodic impulses as

$$\cos\phi \to \cos\phi \times 2\pi\delta_{2\pi}(t), \quad \sin\phi \to \sin\phi \times 2\pi\delta_{2\pi}(t - \pi/2). \tag{20}$$

The new Hamiltonian can now be solved easily from $t = 0$ to $t = 2\pi$ and in this way a mapping is obtained, which is a model for the Poincaré map of the elliptic restricted three body problem at integral multiples of the period 2π of Jupiter's orbit (stroboscobic map). Note that all periodic

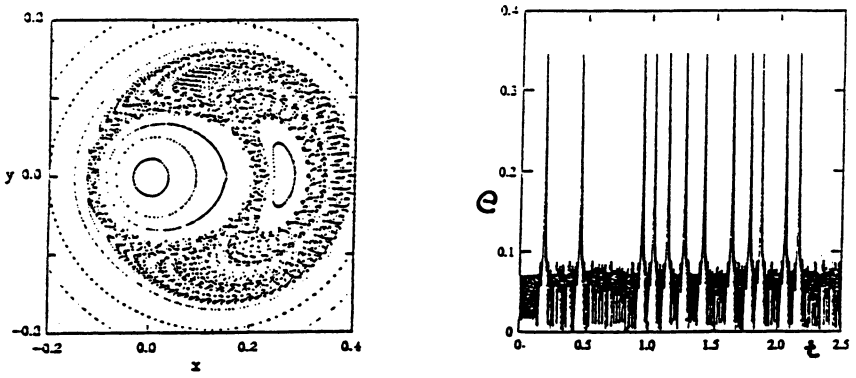

Figure 1. (a):The evolution in the xy plane. The distance from $(0,0)$ is proportional to the eccentricity. (b):The time evolution of the eccentricity (from Wisdom).

orbits in the elliptic restricted three body problem have a period equal to 2π, or a multiple of it. It turns out that this mapping is symplectic. This is a four dimensional map in the space ϕ, Φ, x, y and it is not easy to present geometrically. In this case however, we can further reduce the map to a two dimensional one by taking advantage of the fact that after the averaging we still have a "fast" and a "slow" angle, and we eliminate the fast angle by a new averaging. The fast angle is the resonant angle ϕ, compared to the argument of perihelion ω which is much slower. This is equivalent to taking a "mapping" of the mapping, for example by the "surface of section" H =constant, $\phi = \pi$. In this way we finally obtain a two dimensional map in the space x y.

The evolution of an asteroid at the 3:1 resonance, obtained by this mapping, is shown in Figure 1. We note that there is a large chaotic region and the asteroid may be locked in a motion with small radius (eccentricity) but suddenly may jump to a motion where the radius takes large values. This is clearly seen in Figure 1b, where the eccentricity jumps to values higher than 0.3 at unpredictable times, showing an intermittent behaviour. In this way Wisdom explained the observed gap in the distribution of the asteroids at the 3:1 resonance, because for $e > 0.3$ the asteroid becomes a Mars crosser and the resulting perturbation will remove the asteroid from the 3:1 resonance region.

The Wisdom method has been applied by Šidlichovský (1988, 1990, 1992, 1993) and by Murray and Fox (1984).

6.2. RESONANT ASTEROID MOTION: HADJIDEMETRIOU'S METHOD

The method discussed in section 5.2 has been applied by Hadjidemetriou (1991,1993) for the study of asteroid motion at the 3:1 resonance. The

https://doi.org/10.1017/S0074180900127500 Published online by Cambridge University Press

starting point is also the averaged Hamiltonian of the elliptic restricted three body problem, which is of the form

$$H = H_0(S,N) + \mu H_1(\sigma,S,N) + \mu e_j H_2(\sigma,S,\nu,N), \tag{21}$$

where

$$\begin{aligned} H_0 &= -\frac{2(1-\mu)^2}{(N-S)^2} - \frac{3}{2}(N-S),\ H_1 = 2FS - b\frac{S}{N}\cos 2\sigma, \\ H_2 &= \sqrt{2S}[G\cos(\sigma+\nu) + D\cos(\sigma-\nu)] + 2\mu e_j K\cos 2\nu. \end{aligned}$$

The resonance action-angle variables are defined by

$$S = \sqrt{\mu_1 a}\left(1-\sqrt{1-e^2}\right) \quad \sigma = \frac{1}{2}(3\lambda_j - \lambda) - \omega_j$$

$$N = \sqrt{\mu_1 a}\left(3-\sqrt{1-e^2}\right) \quad \nu = -\frac{1}{2}(3\lambda_j - \lambda) + \omega_j$$

where $\mu_1 = 1-\mu$, $e_j = 0.048$, λ, ω, a are the mean longitude, the longitude of perihelion and the semimajor axis, respectively, of the asteroid and the corresponding quantities with subscript j refer to Jupiter. This is in fact the same as the Hamiltonian (18) used by Wisdom. The mapping is obtained from the generating function

$$F = \sigma_n S_{n+1} + \nu_n N_{n+1} + 2\pi H(S_{n+1}, N_{n+1}, \sigma_n \nu_n), \tag{22}$$

though the equations

$$\sigma_{n+1} = \partial F/\partial S_{n+1},\ S_n = \partial F/\partial \sigma_n,\ \nu_{n+1} = \partial F/\partial N_{n+1},\ N_n = \partial F/\partial \nu_n.$$

and is evidently symplectic.

We can verify that the first two equations are decoupled from the other two if $e_j = 0$. The mapping in this case (*circular* restricted three body problem) is two dimensional, in the space σ, S, with N as a parameter. For different values of N we have different surfaces of section, but no chaotic regions appear. As soon however as $e_j \neq 0$, the parameter N varies slowly and as a consequence a slow drift appears from one N = constant plane to the next. This is the mechanism by which large scale chaos appears (Hadjidemetriou 1993,1995). This mechanism is also given by Wisdom (1985) and Henrard (1992), using the averaged model. The evolution of an asteroid inside the 3:1 resonance is given in Figure 2 for different initial values of σ and ν. The behaviour is in fact the same as that given in Figure 1. (Note the similarity between Figures 1a and 2a). Not all motions however inside the resonance zone are chaotic. We also have ordered motion, as shown in

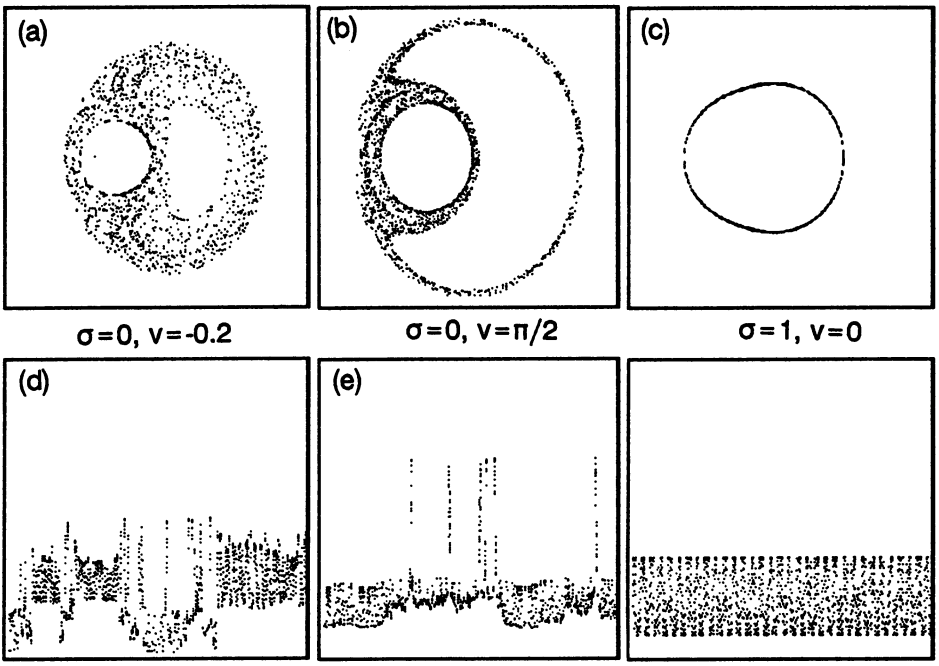

Figure 2. The evolution of an asteroid by the mapping obtained from the generating function (22) for $S = 0.0116$, $N = 1.4$ and σ, ν as indicated: a,b and c give the evolution in the xy plane, and d,e,f the corresponding time evolution of the eccentricity

Figures 2c,f , where we have an oscillation with an amplitude which depends on the initial angles and may be quite small (as is the case with $\sigma = 0$, $\nu = \pi$). This means that we may have a trapping of the asteroid inside the 3:1 resonance.

This method of constructing mapping models has been also used by Ji-Liu et al.(1994) for near conservative systems and by Ferraz-Mello (1995) for the 2:1 resonance.

6.3. REMARKS ON THE PREVIOUS TWO MAPPINGS

The general behaviour of both mappings is the same, as far as the long term evolution is concerned. However both models have their limitations, as we shall explain:

- The averaged model on which these two mapping models are based is valid only for values of the eccentricity smaller than 0.3. This means that the high eccentricity resonances that exist in the real problem (the elliptic restricted three body problem) at eccentricities $e = 0.8$ are missing (Hadjidemetriou 1992). These high eccentricity resonances can be introduced to the system

through a *correction term* (Hadjidemetriou 1993). The corrected mapping behaves in a much different way and the eccentricity can jump to very high values of the eccentricity, 0.9 or even larger. The asteroid can become now an Earth crosser.

-Both models are not realistic for the long time study of asteroid motion, because the orbit of Jupiter is fixed. The elements of Jupiter's orbit vary considerably, as shown by Laskar (1990) and Nobili et al.(1989). If this variation is introduced in the mapping (22), by varying e_j and ω_j, we find (Hadjidemetriou 1993, 1995) that the chaotic behaviour appears for all values of the angles σ and ν, including those cases where the motion was ordered for a fixed orbit of Jupiter, while no appreciable effect appears outside the resonance zone.

Thus, we see that the gravitational effect of Saturn must also be included in the model in order to explain the observed gap in the distribution of the asteroids at the 3:1 resonance.

6.4. OTHER MAPPING TECHNIQUES

6.4.1. *Nearly parabolic orbits*

Mapping models for nearly parabolic orbits have been developed by several people, with the aim to study cometary motion. They are all in the framework of the restricted circular three body problem, with the Sun and Jupiter as primaries. For a nearly parabolic orbit we can assume that the motion is close to the separatrix. Due to the very large time scales (the period of the parabolic orbit is infinite), a Fourier analysis is made and the spectrum is assumed to be continuous. In this way Petrosky and Broucke (1988) transformed the nonintegrable system to an integrable one by embedding the small denominators in an analytic function through a suitable analytic continuation. The corresponding mapping is called *Keplerian map* and is a two dimensional symplectic map in the space P, g, where P is the heliocentric energy of a comet and g the phase angle of Jupiter when the comet is at perihelion. Similar work on the Keplerian map has been made by Chambers (1993), Chirikov and Vecheslavov (1988), Sagdeev and Zaslansky (1987) and Liu and Yi-Sui Sun (1994).

6.4.2. *Nearly circular orbits*

This technique has been developed by Duncan et al.(1989) for the study of a test particle in nearly circular orbit, in the framework of the *circular* restricted three body problem, with the Sun and a planet as primaries. The perturbation on the test particle is assumed to be significant only at conjunction. Under this assumption, the first order perturbation on the elements of the orbit are obtained by Hill's equation. In this way an ap-

proximate solution is found, from which a mapping is obtained.

References

Chambers, J. E.: (1993) "A simple mapping for comets in resonance". *Celest, Mech,* **57**, 131.

Chirikov, B. V. and Vecheslavov, V. V.:(1986) "Chaotic dynamics of comet Haley". preprint 86-184, Institute of Nuclear Physics, Novosibirsk.

Duncan, M., Quinn, T. and Tremaine, S.: (1989) "The long term evolution of orbits in the Solar System: A mapping approach". *Icarus* **82**, 402.

Ferraz-Mello, S.: (1995) preprint.

Froeschlé, C.: (1991) "Modelling: An aim and a tool for the study of the chaotic behaviour of asteroidal and cometary orbits". In *Predictability, Stability and Chaos in N-Body Dynamical Systems*, A. E. Roy (ed), Plenum Press, p. 125-155.

Hadjidemetriou, J. D.: (1991) "Mapping Models for Hamiltonian Systems with application to Resonant Asteroid Motion". In *"Predictability, Stability and Chaos in N-Body Dynamical Systems*, A. E. Roy (ed), Kluwer Publ., p. 157-175.

Hadjidemetriou, J. D.: (1992) "The Elliptic Restricted Problem at the 3:1 Resonance". *Celest. Mech.* **53**, 151-183.

Hadjidemetriou, J. D.: (1993) "Asteroid Motion near the 3:1 Resonance". *Celest. Mech.* **56**, 563-599.

Hadjidemetriou, J. D. and Voyatzis, G.: (1993) "Long Term Evolution of Asteroids near a Resonance". *Celest. Mech.* **56**, 95-96.

Hadjidemetriou, J. D.: (1995), "Mechanisms of Generation of Chaos in the Solar System". In *"From Newton to Chaos*, A. E. Roy and B. A. Steves, (eds), Plenum Press, 79.

Henrard, J.: (1995) private communication.

Henrard, J.: (1988) "Resonances in the Planar Elliptic Restricted Problem". In *Long Term Dynamical Behaviour of Natural and Artificial N-Body Systems*, A. E. Roy (ed), 405- 425, Kluwer Publ.

Ji-Lin Zhou, Yan-Ning Fu and Yi-Sui Sun: (1994) " Mapping models for near-conservative systems with applications". *Celest. Mech.* **60**, 471.

Laskar, J.: (1990) "The chaotic motion of the Solar System". *Icarus* **88**, 266-291.

Liu Jie and Yi-Sui Sun: (1994) "Chaotic motion of comets in near-parabolic orbit: mapping approaches". *Celest. Mech.* **60**, 3.

Nobili, A., Milani, A., Carpino, M.: (1989) "Fundamental Frequencies and Small Divisors in the Orbits of The Outer Planets". *Astron. Astrophys.* **210**, 313-336.

Murray, C. D. and Fox, K.: (1984) "Structure of the 3:1 Jovian resonance: A comparison of numerical methods". *Icarus* **59**, 482.

Petrosky, T. Y. and Broucke, R.: (1988) "Area-preserving mappings and deterministic chaos for nearly parabolic orbits". *Celest. Mech.* **42**, 53.

Sagdeev, R. Z. and Zaslavsky, G. M.: (1987), *Nuovo Cimento* **97**, BN2.

Šidlichovský, M.: (1988), "On the Origin of 5/2 Kirkwood Gap" In *Proceedings of the IAU Colloq. 96, The Few Body Problem* (Turku), Valtonen, M. (ed.), p. 117.

Šidlichovský, M.: (1990), "The Existence of a Chaotic Region Due to the Overlap of Secular Resonances ν_5 and ν_6". *Celes. Mech. Dyn. Astr.* **49**, 177.

Šidlichovský, M.: (1992) "Mapping for the asteroidal resonances". *Astron. Astrophys.* **259**, 341-348.

Šidlichovský, M.: (1993) "Chaotic Behaviour of Trajectories for the Fourth and Third Order Asteroidal Resonances". *Celest. Mech.* **56**, 143.

Wisdom, J.: (1982) "The origin of the Kirkwood Gaps". *Astron. J.* **87**, 577-593.

Wisdom, J.: (1983) "Chaotic Behaviour and the Origin of the 3/1 Kirkwood Gap". *Icarus* **56**, 51-74.

Wisdom, J.: (1985) "A Perturbative Treatment of Motion Near the 3/1 Commensurability". *Icarus* **63**, 272-289.